

First lattice QCD estimate of the $g_{D^*D\pi}$ coupling

A. ABADA^a, D. BEĆIREVIĆ^b, PH. BOUCAUD^a, G. HERDOIZA^a,
J.P. LEROY^a, A. LE YAOUANC^a, O. PÈNE^a,
J. RODRÍGUEZ-QUINTERO^c

^a *Laboratoire de Physique Théorique (Bât.210), Université de Paris XI,
Centre d'Orsay, 91405 Orsay-Cedex, France.*

^b *Dipartimento di Fisica, Università di Roma "La Sapienza",
Piazzale Aldo Moro 2, I-00185 Rome, Italy.*

^c *Dpto. de Física Aplicada, E.P.S. La Rábida, Universidad de Huelva,
21819 Palos de la fra., Spain*

June 24 2002

Abstract

We present the results of the first lattice QCD study of the strong coupling $g_{D^*D\pi}$. From our simulations in the quenched approximation, we obtain $g_{D^*D\pi} = 18.8 \pm 2.3_{-2.0}^{+1.1}$ and $\hat{g}_c = 0.67 \pm 0.08_{-0.06}^{+0.04}$. Whereas previous theoretical studies gave different predictions, our result favours a large value for \hat{g}_c . It agrees very well with the recent experimental value by CLEO. \hat{g} varies very little with the heavy mass and we find in the infinite mass limit $\hat{g}_\infty = 0.69(18)$.

PACS: 12.38.Gc (Lattice QCD calculations), 13.75.Lb (Meson-meson interactions)

1 Introduction

Recent measurement of the full width of the charged D^* -meson, $\Gamma(D^{*+}) = 96 \pm 4 \pm 22$ keV [1], allowed for the experimental determination of the strong coupling of D -mesons to the P -wave pion $g_{D^*D\pi}$, namely

$$g_{D^*D\pi} = 17.9 \pm 0.3 \pm 1.9, \quad \text{i.e. } \hat{g} = 0.59 \pm 0.07, \quad (1)$$

where the definition of \hat{g} in [1] is quoted below. This coupling has been extensively studied in the literature¹, with a variety of approaches : model independent approaches, the QCD sum rules, the quark models.

Model independent approaches [2, 3] have produced windows or bounds which have been confirmed by experiment eq. (1). By the way a rigorous bound $\hat{g} < 1$ is set by the Adler-Weisberger sum rule [4, 5]. Notice that $\hat{g} = 1$ is the naive non relativistic quark model result, to be lowered by relativistic corrections.

The various *QCD sum rules* have been discussed with much care before and after the measurement in eq. (1) and have shown a surprising convergence towards a very low value, almost a factor two below eq. (1), see [6]. In particular, in [7], a value $g_{D^*D\pi} = 10.5 \pm 3.0$ has been quoted. No convincing explanation has been found for this discrepancy.

Quark models, on the contrary, can accommodate large values. Good predictions have been produced, prior to the experimental measure [8, 5]. But there is a large spectrum of predictions 0.3-0.8, corresponding to a multiplicity of models or choice of parameters, therefore one can wonder whether successes are truly significant, or rather due to a happy choice. Without entering into details, one can answer as follows:

1) Light-front quark models have indeed a large range of predictions 0.3-0.8, mainly because they use free quark Dirac spinors, which yield relativistic corrections very sensitive to the choice of the ill-determined light quark mass.

2) Dirac type models, on the contrary, yield naturally large values of $\hat{g} \geq 0.6$, because anyway, a large effective mass is generated for the light quark through the potential [5]. These authors find $\hat{g} = 0.6$. Too large values obtained in other calculations can be corrected by a quark current renormalisation factor, but one loses predictive power.

Before claiming that the QCD based evaluations for this coupling are in conflict with the experimental value, it is important to compute this coupling by employing the lattice QCD simulations, as recently suggested in ref. [11]. An exploratory lattice calculation has been performed in ref. [12] but in the static limit of the heavy quark effective theory (HQET). Here we will directly work in QCD with relativistic propagating quarks since, contrary to the case of b -physics, currently accessible lattices allow to accommodate the charm quark mass and therefore no heavy quark extrapolation is needed. This makes the lattice study of $g_{D^*D\pi}$ rather clean.

In this paper, we report the first calculation of this type in which we used the (improved) Wilson fermions. Our final result at $\beta = 6.2$ is

$$g_{D^*D\pi} = 18.8 \pm 2.3^{+1.1}_{-2.0}, \quad (2)$$

¹ A rather exhaustive list of results for this coupling can be found in [5, 9]. To the references listed there, one should add also ref. [10].

thus in a very good agreement with experiment. The small value predicted by the QCD sum rule still needs an explanation.

The value of the coupling $g_{D^*D\pi}$ provides also the access to the \widehat{g} -coupling which is one of the main parameters of the approach based on the use of chiral perturbation theory for the heavy-light systems. \widehat{g} is related to $g_{D^*D\pi}$ through

$$g_{D^*D\pi} = \begin{cases} 2m_{D^*} \widehat{g}_c / f_\pi & [1] , \\ 2\sqrt{m_D m_{D^*}} \widehat{g}_c / f_\pi & [5] , \\ 2m_D \widehat{g}_c / f_\pi & [13] , \end{cases}$$

where we use $f_\pi = 132$ MeV. All the above definitions coincide up to $1/m_c$ corrections. Throughout this paper we will use the most symmetric definition [5]. Notice that we assigned a subscript c , to stress that the \widehat{g} is not obtained with the infinitely heavy quark (mesons), but rather from the (not-so-heavy) charmed heavy-light mesons. By using the definition [5], from our result (2), we obtain

$$\widehat{g}_c = 0.67 \pm 0.08_{-0.06}^{+0.04} . \quad (3)$$

We performed the simulations at two values of the lattice spacing ($\beta = 6.0$ and $\beta = 6.2$) to study the systematic effects which are discussed in section 6. The simulation was firstly done at $\beta = 6.0$ and will be summarized in section 5. Our main results are given from the simulations at $\beta = 6.2$ since they have smaller $\mathcal{O}(a)$ -effects. This analysis is detailed in sections 2 to 4.

2 Lattice parametrization and results of the analysis of the two-point functions

The main results presented in this paper and detailed in this section are obtained from the simulation on a $24^3 \times 64$ lattice with periodic boundary conditions, at $\beta = 6.2$. Our sample contains 100 independent $SU(3)$ gauge configurations produced in the quenched approximation (*i.e.* $n_F = 0$). The quark propagators are computed by using the following Wilson hopping parameters for light (q) and heavy (Q) quarks:

$$\begin{aligned} \kappa_q &= 0.1344_{q_1} , 0.1348_{q_2} , 0.1351_{q_3} ; \\ \kappa_Q &= 0.1250_{Q_1} , 0.1220_{Q_2} , 0.1190_{Q_3} , \end{aligned} \quad (4)$$

where we introduced the labels q_{1-3} and Q_{1-3} that will be used throughout this paper. We have implemented the non-perturbative $\mathcal{O}(a)$ improvement of the Wilson fermion action, by setting $c_{SW} = 1.614$ [14].

In this section we consider the standard two-point correlation functions

$$C_{PP}^{(2)}(t_x; \vec{p}) = \left\langle \sum_{\vec{x}} e^{i\vec{p}\cdot\vec{x}} P(0)P(x) \right\rangle , \quad C_{V_\mu V_\nu}^{(2)}(t_x; \vec{p}) = \left\langle \sum_{\vec{x}} e^{i\vec{p}\cdot\vec{x}} V_\mu(0)V_\nu(x) \right\rangle \quad (5)$$

where $t_x > 0$ and where $P \equiv \bar{q}'\gamma_5 q$ and $V_\mu \equiv \bar{q}'\gamma_\mu q$ which will be used with heavy-light and light-light quarks. We define the constants \mathcal{Z}_P and \mathcal{Z}_V so that

$$C_{PP}^{(2)}(t_x; \vec{p}) \simeq \mathcal{Z}_P \frac{e^{-E_P t_x}}{2E_P}, \quad C_{V_\mu V_\nu}^{(2)}(t_x; \vec{p}) \simeq \mathcal{Z}_V \frac{e^{-E_V t_x}}{2E_V} (\delta_{\mu\nu} - p_\mu p_\nu / p^2). \quad (6)$$

at large t_x , where E_P (E_V) is the ground state pseudoscalar (vector) meson energy.

From the standard study of these two-point light-light correlation functions, we extracted the masses of pseudoscalar (am_P) and vector mesons (am_V), the decay constant (af_P) and the (bare improved) light quark mass ($a\rho$) that we obtain by using the axial Ward identity, $\partial_\mu A_\mu^I = 2\rho P$. In table 1, we list our results for both the degenerate and non-degenerate combinations of our light quarks. In the computation of the pseudoscalar

	am_P	am_V	$a\rho$	af_P^R
$\kappa_{q1} - \kappa_{q1}$	0.306(1)	0.409(3)	0.0413(4)	0.068(2)
$\kappa_{q1} - \kappa_{q2}$	0.284(2)	0.393(4)	0.0354(3)	0.065(2)
$\kappa_{q1} - \kappa_{q3}$	0.266(2)	0.381(4)	0.0310(3)	0.063(2)
$\kappa_{q2} - \kappa_{q2}$	0.259(2)	0.377(5)	0.0296(3)	0.062(2)
$\kappa_{q2} - \kappa_{q3}$	0.240(2)	0.364(5)	0.0252(3)	0.060(2)
$\kappa_{q3} - \kappa_{q3}$	0.219(2)	0.350(6)	0.0208(2)	0.058(2)

Table 1: *Light meson masses, bare quark masses and (renormalized) pseudoscalar decay constants. The time intervals chosen for the fits are: $P : t \in [10, 30]$, $V : t \in [11, 25]$, and $\rho, f_P : t \in [12, 29]$.*

decay constant and of the bare quark mass we improved the axial current at $\mathcal{O}(a)$, *i.e.*

$$A_\mu^I(x) = A_\mu(x) + c_A(g_0^2)\partial_\mu P(x), \quad (7)$$

where $c_A = -0.038(4)$, as determined non-perturbatively at $\beta = 6.2$ in refs. [14, 15, 16]. In the computation of the renormalized decay constant, the $\mathcal{O}(a\rho)$ effects are eliminated by redefining

$$Z_A^I(g_0^2) = Z_A^{(0)}(g_0^2) \left(1 + \tilde{b}_A(g_0^2)a\rho\right), \quad (8)$$

where the non-perturbatively estimated constants are $Z_A^{(0)} = 0.81(1)$ [15, 17, 18], and $\tilde{b}_A = 1.19(6)$ [15].

By using the lattice plane method [21], illustrated in fig. 1, we get $af_\pi = 0.0488(24)$, which after comparison with the physical $f_\pi = 0.132$ GeV, leads to the following value of the inverse lattice spacing:

$$a^{-1}(f_\pi) = 2.71(12) \text{ GeV} . \quad (9)$$

That value is consistent with the one obtained by using the ρ -meson mass ($a^{-1}(m_\rho) = 2.62(9)$ GeV) and/or the K^* -meson ($a^{-1}(m_{K^*}) = 2.67(8)$ GeV).

As for the heavy-light systems, in what follows, we will need the pseudoscalar and vector meson masses, in addition to the constants $\mathcal{Z}_P, \mathcal{Z}_V$ (6). We obtain those quantities by fitting our lattice results for the correlators (5) with the mesons at rest ($\vec{p} = 0$), to the forms given in eq.(6). The results are presented in table 2.

	am_P	am_V	\mathcal{Z}_P	\mathcal{Z}_V
$\kappa_{Q_1} - \kappa_{q_1}$	0.692(2)	0.732(2)	0.0187(9)	0.0068(4)
$\kappa_{Q_1} - \kappa_{q_2}$	0.678(2)	0.719(3)	0.0176(9)	0.0062(5)
$\kappa_{Q_1} - \kappa_{q_3}$	0.669(2)	0.710(4)	0.0171(10)	0.0059(6)
$\kappa_{Q_2} - \kappa_{q_1}$	0.788(2)	0.822(2)	0.0207(10)	0.0080(5)
$\kappa_{Q_2} - \kappa_{q_2}$	0.775(2)	0.809(3)	0.0195(11)	0.0073(6)
$\kappa_{Q_2} - \kappa_{q_3}$	0.766(3)	0.800(4)	0.0189(12)	0.0070(7)
$\kappa_{Q_3} - \kappa_{q_1}$	0.878(2)	0.907(2)	0.0222(11)	0.0091(6)
$\kappa_{Q_3} - \kappa_{q_2}$	0.866(2)	0.894(3)	0.0208(12)	0.0083(7)
$\kappa_{Q_3} - \kappa_{q_3}$	0.857(3)	0.885(4)	0.0203(13)	0.0079(8)

Table 2: Meson masses and \mathcal{Z} 's in lattice units extracted from our lattice data. Indices in the hopping parameters (q_{1-3} and Q_{1-3}) are specified in eq. (4). The time-intervals used for the fits are $P : t \in [15, 30]$, $V : t \in [17, 28]$.

3 Computation of the three-point functions: Basics and Results

In this section we define the quantities that we need to compute and explain the strategy that will allow us extracting the coupling $g_{VP\pi}$, where P and V stand for the heavy-light vector and pseudoscalar mesons respectively. We will then present our results obtained for the heavy and light quark masses that are directly accessible from our lattice.

3.1 Theoretical basis

We start from the computation of the transition matrix element between the heavy-light vector meson (V) and the heavy-light pseudoscalar (P), mediated by the axial light-light current $A_\mu = \bar{q}\gamma_\mu\gamma_5q$ (see fig. 2). It is parametrized as

$$\begin{aligned} \langle P(p') | A^\mu | V(p, \lambda) \rangle &= 2m_V A_0(q^2) \frac{\epsilon^\lambda \cdot q}{q^2} q^\mu + (m_P + m_V) A_1(q^2) \left[\epsilon^{\lambda\mu} - \frac{\epsilon^\lambda \cdot q}{q^2} q^\mu \right] \\ &\quad + A_2(q^2) \frac{\epsilon^\lambda \cdot q}{m_P + m_V} \left[p^\mu + p'^\mu - \frac{m_V^2 - m_P^2}{q^2} q^\mu \right] \end{aligned} \quad (10)$$

where $q = p - p'$ ². The matrix element of the divergence $q_\mu A^\mu$ is dominated by the pion pole for q^2 in the vicinity of m_π^2 :

$$\langle P(p') | q_\mu A^\mu | V(p, \lambda) \rangle = g_{VP\pi} \frac{\epsilon^\lambda(p) \cdot q}{m_\pi^2 - q^2} \times f_\pi m_\pi^2 + \dots \quad (11)$$

From eq. (11), we find for $q^2 = 0$:

$$g_{VP\pi} = \frac{2m_V A_0(0)}{f_\pi}. \quad (12)$$

With our settings, the lattice transfer at $\vec{q} = \vec{0}$ happens to be close to $q^2 = 0$ (see table 3). However, the lattice simulations at $\vec{q} = \vec{0}$ can only give the form factor A_1 . The other ones, $A_{0,2}$, can be computed at $\vec{q} \neq \vec{0}$ which in our case is no longer close to $q^2 = 0$, as can be seen in table 3. Since A_0 has the pion pole, it varies very fast in the vicinity of $q^2 = 0$ and thus cannot be directly extrapolated. To overcome this difficulty, we express $A_0(0)$ in terms of $A_{1,2}(0)$ which do not have a pion pole. This relation can be obtained by using the fact that in eq. (10), the axial current cannot have a singularity at $q^2 = 0$. The three residues of $1/q^2$ -terms must cancel, this leads to:

$$g_{VP\pi} = \frac{1}{f_\pi} \left[(m_V + m_P) A_1(0) + (m_V - m_P) A_2(0) \right]. \quad (13)$$

In this relation, one can see that the A_1 contribution is dominant. This dominant contribution is directly obtained from lattices at $\vec{q} = \vec{0}$, as already mentioned. A_2 has to be extrapolated from $\vec{q} \neq \vec{0}$ to $q^2 = 0$. Its nearest pole is the a_1 meson mass. The error generated with this extrapolation will be discussed in the next subsection. This error is anyhow harmless since it applies only to the subdominant contribution ($\lesssim 5\%$) to $g_{VP\pi}$.

In the heavy quark limit ($m_Q \rightarrow \infty$), in which $m_V = m_P$, only the form factor $A_1(0)$ contributes. In that limit one recovers the formula used in ref. [12] to compute this coupling. For heavy quarks close to charm, the corrections in powers of the inverse heavy quark mass are expected to be sizable, which is why we decided to compute $g_{VP\pi}$ with the

² This definition of form factors is equivalent to the usual one : the matrix element $\langle V | A^\mu | P \rangle$ has a “-” sign in front of A_2 .

relativistic (propagating) heavy quark. Notice that isospin symmetry relates various charge combinations of the $VP\pi$ couplings:

$$g_{VP\pi} \equiv g_{V^+P^0\pi^+} = -\sqrt{2}g_{V^+P^+\pi^0} = -g_{V^0P^+\pi^-} . \quad (14)$$

For simplicity, we define

$$G_1(q^2) = \frac{m_V + m_P}{f_\pi} A_1(q^2) , \quad G_2(q^2) = \frac{m_V - m_P}{f_\pi} A_2(q^2) , \quad (15)$$

and rewrite eq. (13) as

$$g_{VP\pi} = G_1(0) \cdot \left(1 + \frac{G_2(0)}{G_1(0)} \right) . \quad (16)$$

As already mentioned $G_1(0)$ is the dominant contribution to $g_{VP\pi}$, the G_2/G_1 being a few percent correction to it.

Analogously, the expression for \widehat{g}_Q at a given heavy quark Q mass is

$$\widehat{g}_Q = \widehat{g}_Q^{(0)} \cdot \left(1 + \frac{G_2(0)}{G_1(0)} \right) , \quad (17)$$

where we note, according to [5],

$$\widehat{g}_Q^{(0)} = \frac{m_V + m_P}{2\sqrt{m_V m_P}} A_1(0) . \quad (18)$$

3.2 Computation of the three point functions

To access the matrix element (10) from the lattice, we compute the following three-point functions

$$C_{\mu\nu}^{(3)}(0, \vec{q}, t_x; \vec{0}, t_y) = \left\langle \sum_{\vec{x}, \vec{y}} V_\mu(0) A_\nu(x) P(y) e^{-i\vec{q}\cdot\vec{x}} \right\rangle_{0 < t_x < t_y} , \quad (19)$$

where the pseudoscalar meson is inserted at rest ($\vec{p}' = (0, 0, 0)$) at a fixed time chosen to be $t_y = 31a$, while the current operator has a momentum $\vec{q} \in \{(0, 0, 0), (1, 0, 0)\}$ in units of the elementary momentum ($2\pi/La \simeq 0.7$ GeV). The vector meson interpolating field is at the origin $(0, \vec{0})$ of the lattice.

When both mesons are at rest, the only useful ratio is ($t \equiv t_x$)

$$R_1(t) = \frac{C_{ii}^{(3)}(t) \mathcal{Z}_V^{1/2} \mathcal{Z}_P^{1/2}}{C_{V_i V_i}^{(2)}(t) C_{PP}^{(2)}(t_y - t)} , \quad (20)$$

which develops a plateau for $t \in [12, 17]$. At that plateau we extract the matrix element (10), *i.e.* the value of the form factor $A_1(q^2)$. To access the ratio A_2/A_1 , we study the ratios with the momentum injection $\vec{q} = (1, 0, 0) \times 2\pi/L$, namely

$$R_2(t) = \frac{C_{10}^{(3)}(t; \vec{q}) \mathcal{Z}_V^{1/2} \mathcal{Z}_P^{1/2}}{C_{V_2 V_2}^{(2)}(t; \vec{q}) C_{PP}^{(2)}(t_y - t)} ,$$

$$\begin{aligned}
R_3(t) &= \frac{C_{11}^{(3)}(t; \vec{q}) \mathcal{Z}_V^{1/2} \mathcal{Z}_P^{1/2}}{C_{V_2 V_2}^{(2)}(t; \vec{q}) C_{PP}^{(2)}(t_y - t)}, \\
R_4(t) &= \frac{C_{22}^{(3)}(t; \vec{q}) \mathcal{Z}_V^{1/2} \mathcal{Z}_P^{1/2}}{C_{V_2 V_2}^{(2)}(t; \vec{q}) C_{PP}^{(2)}(t_y - t)}. \tag{21}
\end{aligned}$$

After inspecting the ratios (21) for all the combinations of heavy and light quarks, we choose to fit them to a plateau at $t \in [14, 17]$. We illustrate in fig. 3 the signals for all the four ratios for a given κ_Q, κ_q . We notice that the ratio $R_2(t)$ has a hardly observable plateau, the value of which is compatible with zero. As just stated the ratio $R_1(t)$ contributes more than 95% to g_{VPp} and its plateau is very good.

Denoting r_i the average value of R_i on the plateaus, the form factors $A_{1,2}$ are then given by :

$$A_1(\vec{q} = \vec{0}) = -\frac{r_1}{m_V + m_P}, \quad A_1\left(\vec{q} = \frac{2\pi}{L}(1, 0, 0)\right) = -\frac{r_4}{m_V + m_P}, \tag{22}$$

$$\frac{A_2}{A_1} = \frac{(m_P + m_V)^2}{2m_P^2 \vec{q}^2} \left[(\vec{q}^2 - E_V(E_V - m_P)) + \frac{m_V^2(E_V - m_P)}{E_V} \frac{r_3}{r_4} + i \frac{m_V^2 q_1}{E_V} \frac{r_2}{r_4} \right], \tag{23}$$

where E_V is the energy of the vector meson.

Our numerical simulations indicate that the ratio A_2/A_1 is positive and of the order of 1. It results from eq. (15) that $G_2/G_1 \sim (m_V - m_P)/(m_V + m_P)$ which leads to a small and positive correction to $G_1(0)$ in (16).

In the left part of table 3, we present our results for the form factor $A_1(q^2)$ ($G_1(q^2)$) for all the quark combinations and with both mesons at rest, $q^2 = (m_V - m_P)^2$. In this case, $q^2 \in (0.04, 1.16) \cdot 10^{-2} \text{ GeV}^2$. They are obviously very close to zero and it is reasonable to assume that, at such small q^2 , $G_1(q^2) \simeq G_1(0)$.

The results for the ratios of the form factors A_2/A_1 (or, equivalently, G_2/G_1) with $\vec{q} = (1, 0, 0) \times 2\pi/L$ are listed in the right part of table 3. They are obtained from the ratios r_{2-4} (see eq. (23)). As expected, the ratios of the form factors G_2/G_1 are positive and very small (they never exceed 5%). Now this ratio has to be extrapolated to $q^2 = 0$. The $A_{1,2}$ form factors may change significantly but without changing sign since the nearest pole, the a_1 -meson, lies at larger q^2 ($m_{a_1} \approx 1.2 \text{ GeV}$ [19])³. On the other hand, the ratio A_2/A_1 is expected to be rather constant because $A_{1,2}$ have the same pole factor $1/(1 - q^2/m_{a_1}^2)$ which cancels out in the ratio⁴. We thus extrapolate A_2/A_1 by keeping this ratio constant.

³ This is confirmed by the ratio $r_4/r_1 = A_1(\vec{q} = (1, 0, 0) \times 2\pi/L)/A_1(\vec{q} = \vec{0}) \sim 0.6$.

⁴ $1/(1 - q^2/m_{a_1}^2)$ varies of about 30% – 40% since for $\vec{q} = (1, 0, 0) \times 2\pi/L$, $q^2 \in (-0.48, -0.44) \text{ GeV}^2$.

	$\vec{q} = (0, 0, 0)$			$\vec{q} = (1, 0, 0) \times 2\pi/L$		
	$q^2 \times 10^{-2} \text{ GeV}^2$	$A_1(q^2)$	$G_1(q^2)$	$q^2 \times 10^{-2} \text{ GeV}^2$	A_2/A_1	G_2/G_1
$\kappa_{Q_1} - \kappa_{q_1} - \kappa_{q_1}$	1.17(17)	0.71(4)	14.9 ± 0.9	-44.8(3.9)	0.85(14)	0.024(4)
$\kappa_{Q_1} - \kappa_{q_1} - \kappa_{q_2}$	0.52(12)	0.68(6)	14.8 ± 1.2	-46.3(4.0)	0.74(12)	0.014(2)
$\kappa_{Q_1} - \kappa_{q_1} - \kappa_{q_3}$	0.23(10)	0.68(6)	15.1 ± 1.3	-47.1(4.1)	0.70(19)	0.009(2)
$\kappa_{Q_1} - \kappa_{q_2} - \kappa_{q_2}$	1.20(22)	0.69(5)	15.5 ± 1.2	-44.7(3.9)	0.93(22)	0.027(6)
$\kappa_{Q_1} - \kappa_{q_2} - \kappa_{q_3}$	0.73(21)	0.67(7)	15.5 ± 1.5	-45.7(3.9)	0.85(25)	0.019(5)
$\kappa_{Q_1} - \kappa_{q_3} - \kappa_{q_3}$	1.24(30)	0.68(5)	16.0 ± 1.5	-44.5(3.8)	1.13(35)	0.034(9)
$\kappa_{Q_2} - \kappa_{q_1} - \kappa_{q_1}$	0.82(12)	0.71(4)	16.9 ± 1.1	-46.1(4.1)	0.89(14)	0.018(3)
$\kappa_{Q_2} - \kappa_{q_1} - \kappa_{q_2}$	0.31(9)	0.68(6)	16.7 ± 1.4	-47.3(4.2)	0.77(14)	0.010(2)
$\kappa_{Q_2} - \kappa_{q_1} - \kappa_{q_3}$	0.11(7)	0.68(6)	17.1 ± 1.5	-48.0(4.2)	0.73(22)	0.006(2)
$\kappa_{Q_2} - \kappa_{q_2} - \kappa_{q_2}$	0.84(17)	0.69(5)	17.5 ± 1.5	-46.0(4.0)	1.19(22)	0.025(4)
$\kappa_{Q_2} - \kappa_{q_2} - \kappa_{q_3}$	0.47(16)	0.68(7)	17.7 ± 1.7	-46.9(4.1)	0.92(29)	0.015(4)
$\kappa_{Q_2} - \kappa_{q_3} - \kappa_{q_3}$	0.85(24)	0.68(6)	18.3 ± 1.8	-45.9(3.9)	1.27(38)	0.028(7)
$\kappa_{Q_3} - \kappa_{q_1} - \kappa_{q_1}$	0.60(9)	0.71(4)	18.9 ± 1.3	-46.9(4.2)	0.93(14)	0.015(2)
$\kappa_{Q_3} - \kappa_{q_1} - \kappa_{q_2}$	0.19(6)	0.68(7)	18.5 ± 1.7	-48.0(4.2)	0.80(15)	0.007(1)
$\kappa_{Q_3} - \kappa_{q_1} - \kappa_{q_3}$	0.04(5)	0.68(7)	19.1 ± 1.8	-48.7(4.3)	0.78(25)	0.003(1)
$\kappa_{Q_3} - \kappa_{q_2} - \kappa_{q_2}$	0.61(14)	0.70(5)	19.6 ± 1.7	-46.9(4.1)	1.08(23)	0.018(4)
$\kappa_{Q_3} - \kappa_{q_2} - \kappa_{q_3}$	0.62(20)	0.68(7)	19.9 ± 2.1	-47.7(4.2)	1.00(32)	0.012(3)
$\kappa_{Q_3} - \kappa_{q_3} - \kappa_{q_3}$	0.25(8)	0.68(6)	20.5 ± 2.2	-46.9(4.1)	1.43(41)	0.024(6)

Table 3: $A_1, G_1, A_2/A_1, G_2/G_1$ at $\beta = 6.2$ for several values of q^2 in the physical units (GeV^2) as obtained by using $a^{-1} = 2.71(12) \text{ GeV}$ (from eq. (9)).

3.3 Comment about the effect of improvement on the form factors

As a side remark, we comment on the effect of the improvement of the bare axial current (see eq. (7)) on the form factors $A_{1,2,0}(q^2)$. The divergence of the current in the matrix element (10) leads to

$$\langle P(p') | \bar{q} \gamma_5 q | V(p, \lambda) \rangle = 2m_V \frac{(e_\lambda \cdot q)}{2\rho_q} A_0(q^2), \quad (24)$$

where we used eq. (10) and the axial Ward identity, $\partial_\mu A_\mu^I = 2\rho_q P$. Therefore the improvement will only affect the form factor $A_0(q^2)$, but not the other two ($A_{1,2}(q^2)$). In other words,

$$\begin{aligned} A_{1,2}(q^2) &\rightarrow A_{1,2}^I(q^2) = A_{1,2}(q^2), \\ A_0(q^2) &\rightarrow A_0^I(q^2) = \left(1 - c_A \frac{q^2}{2\rho_q}\right) A_0(q^2). \end{aligned} \quad (25)$$

As our method to compute $g_{D^*D\pi}$ relies on the computation of the form factors A_1 and A_2 only, our result does not depend at all on the improvement of the bare axial current.

4 Chiral extrapolations and the heavy quark interpolation

Now it is a simple matter to combine our results from table 3 in the way indicated in eq. (16), and to compute the values of the couplings g_{VPp} ⁵. Those numbers should now be extrapolated to the to the physical pion mass, to get $g_{VP\pi}$ for each of our heavy quarks. Finally this is to be followed by interpolation in the heavy meson masses to the ones corresponding to D and D^* .

4.1 Chiral extrapolations

Our light pseudoscalar mesons (“pions”) are rather heavy and we need to extrapolate to the physical pion mass⁶, $m_\pi = 0.14$ GeV. From the lattice planes method [21], the physical pion mass in lattice units is $am_\pi = 0.053(2)$. To obtain $g_{VP\pi}$, we can fit the g_{VPp} -dependence on the quark mass with three formulae:

- Linear extrapolation: by fitting our data to

$$g_{VPp} = a_0 + a_1(am_p)^2, \quad (26)$$

where the values of (am_p) are listed in the first column of table 1. This fit allows to fix the parameters $a_{0,1}$ and thus to extract $g_{VP\pi}$ by either simply reading off a_0 (chiral limit), or by combining $a_{0,1}$ with am_π . We will give results by opting for the latter choice.

⁵ The lower subscript “p” labels the light pseudoscalar meson.

⁶ In physical units, our light pseudoscalar mesons are in the range $m_p \in (0.5, 0.8)$ GeV.

- Quadratic extrapolation: we also attempt the quadratic fit :

$$g_{VPp} = b_0 + b_1(am_p)^2 + b_2(am_p)^4 . \quad (27)$$

- “Chiral Log” extrapolation: One can also fit to a form motivated by the chiral perturbative expansion for the heavy-light systems (for a review, see ref. [13]). In particular, the coupling of the pion to the heavy meson doublet receives logarithmic corrections [22] :

$$g_{VPp} = c_0 + c_1(am_p)^2 + c_2(am_p)^2 \log((am_p)^2) . \quad (28)$$

The results of all three fits are presented in table 4 and illustrated in fig. 4. The quadratic and logarithmic extrapolations are rather unstable i.e. significantly dependent on small changes in the analysis procedure, because we extrapolate from too heavy quark masses. We present them mainly as an estimate of the systematic error.

κ_Q	am_P	am_V	$G_1(0)^{(lin.)}$	$G_1(0)^{(quad.)}$	$G_1(0)^{(log.)}$	$g_{VP\pi}^{(lin.)}$
$Q_1 : 0.1250$	0.645(3)	0.688(6)	16.8 ± 1.9	15.6 ± 2.4	15.0 ± 3.0	17.7 ± 2.2
$Q_2 : 0.1220$	0.744(4)	0.779(6)	19.3 ± 2.4	18.0 ± 3.3	17.2 ± 4.2	20.1 ± 2.7
$Q_3 : 0.1190$	0.836(4)	0.865(7)	21.7 ± 3.0	20.3 ± 4.3	19.3 ± 5.6	22.6 ± 3.3

Table 4: For each heavy quark directly simulated on the lattice we show the values of the heavy-light meson masses for which the light quark is (linearly) extrapolated to the u/d -quark mass. We also list the values of the corresponding $G_1(0)$ (i.e. the $g_{VP\pi}$ coupling without the G_2/G_1 correction) by using eqs. (26, 27, 28), and in the last column, the $g_{VP\pi}$ linearly extrapolated including the G_2/G_1 correction (see eq. (16)).

κ_Q	$\widehat{g}_Q^{(0, lin.)}$	$\widehat{g}_Q^{(lin.)}$
$Q_1 : 0.1250$	0.636(65)	0.669(72)
$Q_2 : 0.1220$	0.641(76)	0.668(79)
$Q_3 : 0.1190$	0.648(86)	0.673(88)

Table 5: For each heavy quark we show the values of $\widehat{g}_Q^{(0)}$ for which the light quark is linearly extrapolated to the u/d -quark mass and the \widehat{g}_Q linearly extrapolated including the $G_2(0)/G_1(0)$ correction (see eq.(17)).

4.2 Chiral extrapolations with two different light quarks

We have computed the three-point Green functions with two different light quark masses m_1, m_2 for the quarks q_1, q_2 shown in fig 2. The form factors extracted from the latter depend, in general, both on $m_2 + m_1$ and $m_2 - m_1$ what makes the chiral extrapolation rather tricky. Luckily, however, it can be shown ⁷ that, in the heavy quark limit, the dominant contribution to $g_{VP\pi}$, *i.e.* $G_1(0)$, only depends on $m_2 + m_1$. In this limit, we can use data with ($m_1 \neq m_2$) to perform our chiral extrapolation as a function of $m_2 + m_1$ (or similarly, as a function of $(m_p)^2$). We have compared the results of the linear extrapolation using this method with the one which uses Green functions with only $m_1 = m_2$. The extrapolated results agree within 2% while the statistical error is typically $\sim 15\%$. Considering six (m_1, m_2) couples allows to estimate the systematic error due to the chiral extrapolation by comparing the linear, quadratic and logarithmic extrapolations as explained in the preceding subsection. As can be seen in table 4, $G_1(0)$ was computed in this way.

The quark mass dependence of the corrective term $G_2(0)/G_1(0)$ in eqs. (16,17) is dominated by the factor $m_V - m_P$ in eq. (15). In the infinite mass limit, it is known that $m_V - m_P \propto m_2 - m_1 + \mathcal{O}(1/m_Q)$. The corrective term $G_2(0)/G_1(0)$ is then dominantly proportional to $m_2 - m_1$ ⁸ and the contributions with $m_1 \neq m_2$ are useless for the chiral extrapolation. Therefore, we have only considered the case $m_1 = m_2$ when including the correction $G_2(0)/G_1(0)$.

4.3 Interpolation to the charm sector

Finally, we need to reach the mass of the charm quark. To that end we will use the values of the spin-averaged masses of the heavy-light mesons

$$\overline{m}_H = \frac{3m_V + m_P}{4} . \quad (29)$$

When converted to the physical units by means of $a^{-1}(f_\pi)$ (given in eq. (9)), we have

$$\overline{m}_H \in \{ 1.83(9), 2.08(10), 2.32(11) \} \text{ GeV} . \quad (30)$$

and $\overline{m}_D = 1.974 \text{ GeV}$ is within this range. The coupling \widehat{g}_Q that we already mentioned in the introduction :

$$g_{VP\pi} = \frac{2\sqrt{m_P m_V}}{f_\pi} \widehat{g}_Q . \quad (31)$$

is the proper parameter to be used for an interpolation in the heavy quark mass. The heavy quark symmetry suggests us to fit our data to the following forms

$$\frac{g_{VP\pi}}{\overline{m}_H} = a_1 + \frac{a_2}{\overline{m}_H} \quad \text{and} \quad \widehat{g}_Q = b_1 + \frac{b_2}{\overline{m}_H} . \quad (32)$$

⁷ Using the heavy quark symmetry and the hermiticity of A_μ , one derives that $\langle V(m_2)|A_\mu|P(m_1) \rangle = \langle P(m_2)|A_\mu|V(m_1) \rangle = \langle V(m_1)|A_\mu|P(m_2) \rangle$.

⁸ We have indeed checked that the slope of $G_2(0)/G_1(0)$ as a function of $m_2 - m_1$ is four times larger than the one as a function of $m_1 + m_2$.

Using these forms we now interpolate to the charm region each of our three sets of chirally extrapolated data from the previous subsection. The results are presented in table 6.

χ -extrap.	$g_{D^*D\pi}$	\widehat{g}_c	\widehat{g}_∞
linear	18.82 ± 2.34	0.669(75)	0.69(18)
quadratic	17.11 ± 3.10	0.574(88)	0.62(27)
χ -log	16.39 ± 4.02	0.551(118)	0.57(37)

Table 6: Results of the linear interpolation of the form (32) to D - D^* mesons at $\beta = 6.2$, for each of the three chiral extrapolations discussed in the text. Note that only the linearly extrapolated result incorporates the G_2/G_1 correction. The other two are uncorrected.

Illustration of that interpolation for the case of the linear chiral extrapolation is provided in fig. 5. Note that our results indicate that the slope in $1/m_H$ for the coupling \widehat{g}_Q is small and negative. Assuming that the linear dependence in $1/m_H$ holds all the way to $1/m_H \rightarrow 0$, we obtain that \widehat{g}_∞ is not more than 15 % larger than \widehat{g}_c (numerical results for \widehat{g}_∞ are also given in table 6).

5 Results at $\beta = 6.0$

In this section we briefly summarize the results obtained at $\beta = 6.0$. The analysis follows the lines presented in the previous sections. We have run in a $16^3 \times 64$ volume over 100 configurations with the following set of light quarks Wilson hopping parameters: $\kappa_q = 0.1339, 0.1342, 0.1344, 0.1346$. We will only show results for one heavy quark, the closest to the physical charm, $\kappa_Q = 0.1190$ ($m_P = 1.77(11)$ GeV), for several values of the light quark mass (see table 7). For $\beta = 6.0$, the ratio $G_2(0)/G_1(0)$ has about 100% error, and we prefer to give the uncorrected result $g_Q^{(0)}$ (see eq. (17)), in table 7.

It is worth noticing that the results at $\beta = 6.0$ agree within errors with those at $\beta = 6.2$. This is illustrated in fig. 6 where we compare the case $\beta = 6.0$, $\kappa_Q = 0.1190$ to $\beta = 6.2$, $\kappa_Q = 0.1250$, which corresponds to approximately the same physical mass of the heavy-light meson ($m_P = 1.77(11)$ GeV and $1.75(9)$ GeV respectively). Notice that the numerical results at $\beta = 6.0$ are more noisy than those at $\beta = 6.2$.

For this reason and also because the lattice spacing at $\beta = 6.0$ implies strong limitations on heavy quark masses, we did not attempt an extrapolation to the charm and even less to the infinite mass limit. Notice nevertheless that the charm mass region is almost reached with $\kappa_Q = 0.1190$ in our setup.

6 Physical results and discussion of errors

	0.1339	0.1342	0.1344	0.1346	κ_{ud}
$G_1(0)$	19.9 ± 2.4	20.8 ± 3.0	22.7 ± 4.3	19.3 ± 4.0	21.4 ± 6.0
$\hat{g}_Q^{(0)}$	0.80(7)	0.80(9)	0.83(12)	0.78(13)	0.80(19)

Table 7: Values of $G_1(0)$ and $\hat{g}_Q^{(0)}$ at $\beta = 6.0$ for one fixed heavy quark: $\kappa_Q = 0.1190$ and several light quarks. The extrapolation to the physical pion mass is presented in the last column.

6.1 Systematic uncertainties

- *Discretisation errors-I:* In our study we implemented the full $\mathcal{O}(a)$ improvement of the Wilson QCD action and the axial current. As we discussed in the text, the improvement of the bare axial current does not influence the value of our $g_{D^*D\pi}$. As for the renormalization constant, we used the non-perturbatively determined value, including the coefficient \tilde{b}_A , which ensures the elimination of the artifacts of $\mathcal{O}(a\rho)$.
- *Discretisation errors-II:* Our calculation has been made at $\beta = 6.2$. With intention to study the $\mathcal{O}(a)$ effects, we have also performed the simulation at $\beta = 6.0$ which has been summarized in the preceding section. The good agreement illustrated in fig. 6 shows a small discretization error. One might wonder if the small decrease of \hat{g} from $\beta = 6.0$ to $\beta = 6.2$ is the sign of a systematic finite a effect. This would then point toward a continuum limit lower than the values quoted here. This difference might also simply be a statistical one since it is smaller than one standard deviation. With only two values of the lattice spacing it is not possible to try a systematic study of the continuum limit and thus to discriminate between these hypotheses. Further studies at different values of β are badly needed. From the experience about similar quantities one might hope that the continuum limit will not be too different from the result at $\beta = 6.2$.
- *Discretisation errors-III:* When interpolating to the charm quark, *i.e.* to the \bar{D} -meson (32), we used the value of the lattice spacing as obtained from the pion decay constant. If the lattice spacing is fixed by the ρ -meson mass, the value of the $g_{D^*D\pi}$ remains practically unchanged. This is not surprising since the slope of $g_{VP\pi}/m_H$ in $1/m_H$ is very small so that the slight change of the position of the $1/\bar{m}_D$ does not make any visible impact on the final result (it increases by $\approx 1\%$).
- *Chiral extrapolations:* This source of uncertainty actually dominates our systematic error bars. This shows up also in the difference between linear, quadratic and logarithmic fits. Indeed, at $\beta = 6.0$ the additional lightest quark ($\kappa = 0.1346$) has been added in order to reduce this error. We decide to take the result of the linear extrapolation as our central value since our data follow rather clearly that form.

The difference between that central value (of the linear extrapolations) and the ones obtained through the quadratic and the “log” fits will be included in the systematic uncertainty.

- *Finite volume effects:* We also studied the finite volume effect by performing two parallel simulations at $\beta = 6.0$, with lattice of size $16^3 \times 64$ and $24^3 \times 64$. To illustrate the net effect, we plot in fig. 7 the ratio of a three-point correlation functions (19) as obtained from the simulations with two lattice volumes and for both heavy-light mesons being at rest. Within our statistics, we do not see any evidence for the presence of finite lattice volume effects. To be conservative, however, we will take into account the observation that the central values are in the interval

$$0.95 \leq \frac{C_{ii}^{(3)}(t; 16^3)}{C_{ii}^{(3)}(t; 24^3)} \leq 1.07, \quad (33)$$

and thus will include 6 % in the systematic error.

- *Quenching effects:* When discussing the chiral extrapolations we also considered the effect of using the leading chiral log behavior. It is important to stress that such a behavior is only valid for the full (unquenched) QCD. In the quenched approximation, however, one encounters the so-called quenched logs which are not of the form $m_p^2 \log(m_p^2)$ as in full QCD but rather divergent, of the form $m_0^2 \log(m_p^2)$. Here m_0 stands for the mass of the η' -meson, which in the quenched theory does not decouple from the octet of light pseudoscalar mesons. One could thus envisage a fit to the form [23]

$$g_{VPp} = c_0 + c_1(am_p)^2 \log(am_p) + c_1^{(quench.)} \log(am_p) + c_2(am_p)^2 + \dots \quad (34)$$

If we had been in the region of very small masses we should have used this form of the fit to determine the coefficient $c_1^{(quench.)}$ and then correct for it when getting the quenched physical results. In our case, however, the meson masses we were able to simulate directly are in the region in which the dependence of g_{VPp} on $(am_p)^2$ is linear as can be seen in fig. 4.

6.2 Conclusion

In this paper, we made the first lattice QCD study of the strong coupling of the pion to the spin-doublet of D -mesons, $g_{D^*D\pi}$. Our results, obtained in the quenched approximation, are in a very good agreement with the recent experimental measurement [1]. Our numbers are much larger than the predictions made by using various QCD sum rule techniques. It is also larger than the previous lattice estimate which has been made in the static limit of the heavy quark effective theory [12] and on a very coarse lattice. The reason for that disagreement remains to be understood. It should be noted that our data suggest that the dependence on the heavy quark mass is very weak and that the static value $\widehat{g}_\infty \gtrsim \widehat{g}_c$. A careful extrapolation to the continuum limit is still needed but, inspired from the experience

with similar quantities, one might hope that the continuum limit will not be too different from the result at $\beta = 6.2$.

On the basis of our results and from the discussion of the systematic uncertainties which we combine in the quadratic sum, we conclude that

$$g_{D^*D\pi} = 18.8 \pm 2.3_{-2.0}^{+1.1}, \quad \text{and} \quad \hat{g}_c = 0.67 \pm 0.08_{-0.6}^{+0.4}, \quad (35)$$

which is the result that we quoted at the beginning of this paper (2,3).

The coupling \hat{g} varies very little with the heavy mass and we find in the infinite mass limit

$$\hat{g}_\infty = 0.69 \pm 0.18. \quad (36)$$

A further improvement of our results includes the increase of the statistical sample, computations with static heavy quarks, computations at larger β (such as $\beta = 6.4$), and most importantly the attempt of an unquenched study of this coupling.

Acknowledgement

We thank V. Lubicz, G. Martinelli, S. Prelovsek, J.-C. Raynal and J. Zupan for precious discussions and comments. This work has been supported in part by the European Network ‘‘Hadron Phenomenology from Lattice QCD’’, HPRN-CT-2000-00145. We have used for this work the APE1000 located in the Centre de Ressources Informatiques (Paris-Sud, Orsay) and purchased thanks to a funding from the Ministère de l’Education Nationale and the CNRS.

References

- [1] S. Ahmed *et al.* [CLEO Collaboration], Phys. Rev. Lett. **87** (2001) 251801, [hep-ex/0108013], A. Anastassov *et al.*, [hep-ex/0108043]. K. K. Gan, [hep-ex/0202012].
- [2] P. L. Cho and H. Georgi, Phys. Lett. B **296**, 408 (1992) [Erratum-ibid. B **300**, 410 (1993)] [arXiv:hep-ph/9209239].
- [3] D. Melikhov and M. Beyer, Phys. Lett. B **452** (1999) 121, [hep-ph/9901261];
- [4] C. A. Dominguez and N. Paver, Z. Phys. C **41**, 217 (1988).
- [5] D. Becirevic and A. Le Yaouanc, JHEP **9903** (1999) 021, [hep-ph/9901431].

- [6] P. Colangelo and A. Khodjamirian, “*At the frontier of particle physics*”, vol. 3, 1495-1576, [hep-ph/0010175].
- [7] A. Khodjamirian, R. Ruckl, S. Weinzierl and O. I. Yakovlev, Phys. Lett. B **457** (1999) 245, [hep-ph/9903421].
- [8] P.J. O’Donnell, Q.P. Xu, Phys. Lett. **B336** (1994) 113, [hep-ph/9406300]; W. Jaus, Phys. Rev. **D53** (1996) 1349.
- [9] P. Singer, Acta Phys. Polon. B **30** (1999) 3849, [hep-ph/9910558];
D. Guetta and P. Singer, Nucl. Phys. Proc. Suppl. **93** (2001) 134, [hep-ph/0009057].
- [10] D. Melikhov and B. Stech, Phys. Rev. D **62** (2000) 014006 [hep-ph/0001113].
J. L. Goity and W. Roberts, Phys. Rev. D **64** (2001) 094007, [hep-ph/0012314];
M. Di Pierro and E. Eichten, Phys. Rev. D **64** (2001) 114004, [hep-ph/0104208];
P. Colangelo and F. De Fazio, [hep-ph/0201305]; F. S. Navarra, M. Nielsen and
M. E. Bracco, Phys. Rev. D **65**, 037502 (2002) [arXiv:hep-ph/0109188].
- [11] P. Roudeau, at the “Lepton-Photon 2001”, Rome, Italy, Jul.2001, [hep-ph/0110397].
- [12] G. M. de Divitiis, L. Del Debbio, M. Di Pierro, J. M. Flynn, C. Michael and J. Peisa
[UKQCD Collaboration], JHEP **9810** (1998) 010, [hep-lat/9807032].
- [13] R. Casalbuoni, A. Deandrea, N. Di Bartolomeo, R. Gatto, F. Feruglio and G. Nardulli,
Phys. Rept. **281** (1997) 145, [hep-ph/9605342].
- [14] M. Luscher, S. Sint, R. Sommer, P. Weisz and U. Wolff, Nucl. Phys. B **491** (1997)
323, [hep-lat/9609035].
- [15] T. Bhattacharya, R. Gupta, W. J. Lee and S. R. Sharpe, Phys. Rev. D **63** (2001)
074505, [hep-lat/0009038], see also [hep-lat/0111001].
- [16] S. Collins, C. T. Davies, G. P. Lepage and J. Shigemitsu [UKQCD collaboration],
hep-lat/0110159, see also [hep-lat/0109036].
- [17] M. Luscher, S. Sint, R. Sommer and H. Wittig, Nucl. Phys. B **491** (1997) 344,
[hep-lat/9611015].
- [18] D. Becirevic, V. Lubicz and G. Martinelli, Phys. Lett. B **524** (2002) 115,
[hep-ph/0107124],
D. Becirevic, V. Lubicz, G. Martinelli and M. Testa, Nucl. Phys. Proc. Suppl. **83**
(2000) 863, [hep-lat/9909039].
- [19] M. Gockeler, R. Horsley, H. Perlt, P. Rakow, G. Schierholz, A. Schiller and P. Stephenson,
Phys. Rev. D **57** (1998) 5562, [hep-lat/9707021].
- [20] T. Kaneko, Nucl. Phys. Proc. Suppl. **106** (2002) 133 [hep-lat/0111005].
- [21] C. R. Allton, V. Gimenez, L. Giusti and F. Rapuano, Nucl. Phys. B **489** (1997) 427,
[hep-lat/9611021].

- [22] A. F. Falk and B. Grinstein, Nucl. Phys. B **416** (1994) 771, [hep-ph/9306310].
- [23] D. Becirevic, S. Prelovsek and J. Zupan, “Quenching errors in $B \rightarrow \pi$ and $B \rightarrow K$ transitions” *in preparation*.

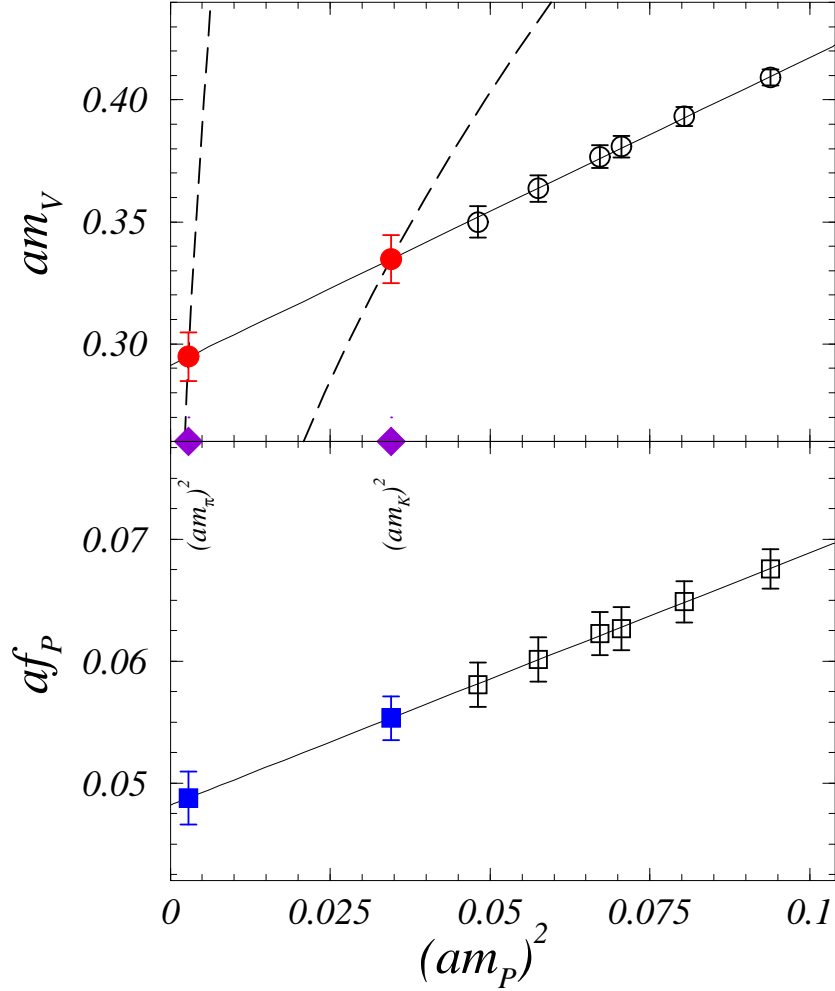


Figure 1: We illustrate the so-called method of lattice planes [21] by which we get the value of $af_{K/\pi}$: In the upper plane, the points in which the fit (solid) line to our data crosses the dashed lines, corresponding to $am_V = C_{K/\pi} \sqrt{(am_P)^2}$ with $C_K = (m_{K^*}/m_K)_{phys}$ and $C_\pi = (m_\rho/m_\pi)_{phys}$ respectively, determine the values of $(am_{K/\pi})^2$, denoted by diamonds. These values are then used to fix $af_{K/\pi}$ (filled squares) in the lower plane, where we fit the pseudoscalar decay constants as $\alpha + \beta(am_P)^2$.

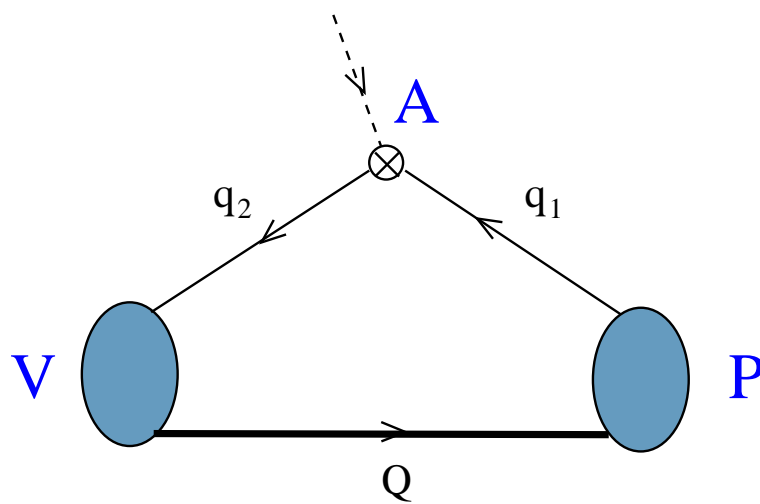


Figure 2: The graph of the three-point function that we compute in this work.

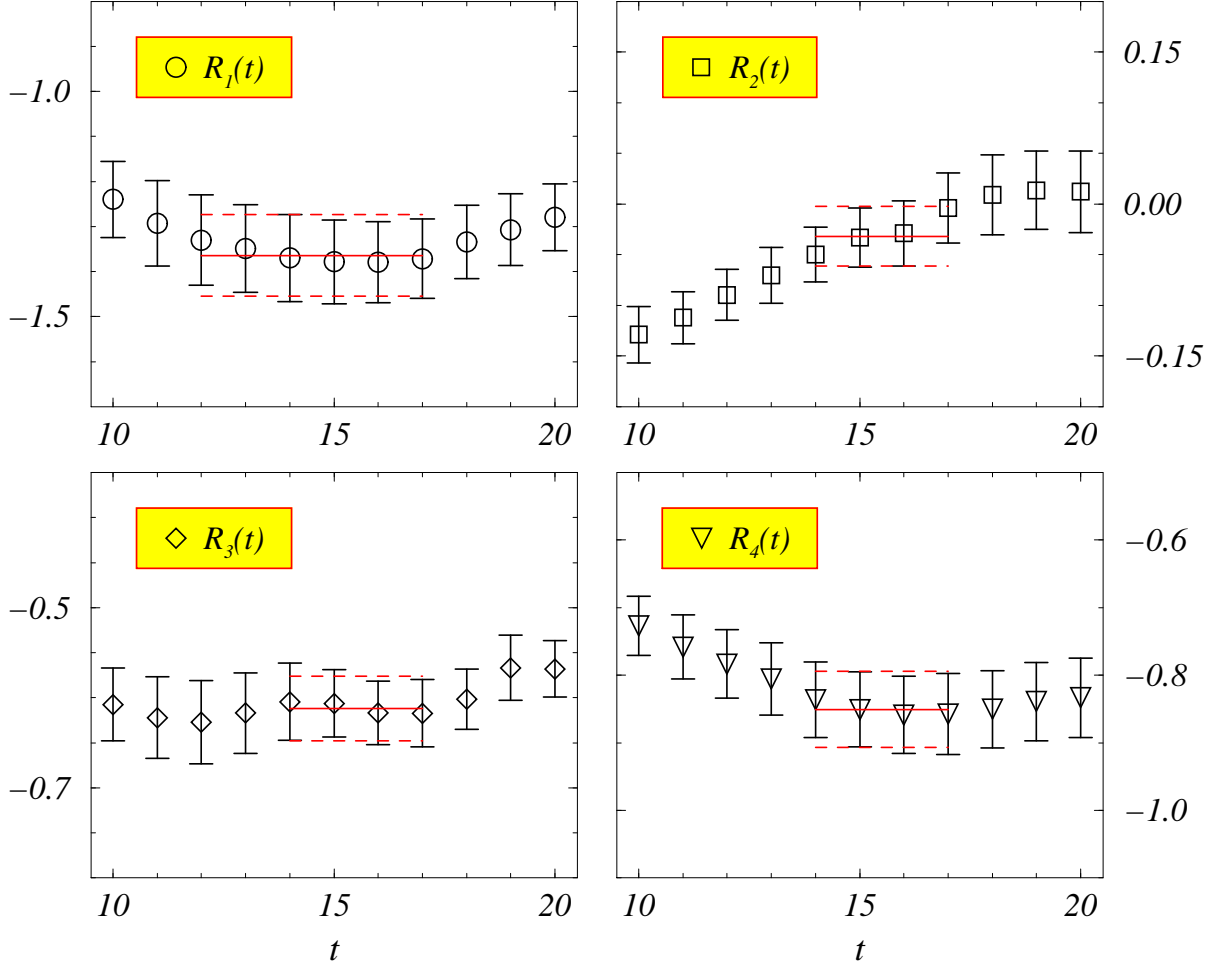


Figure 3: Signals for the ratios $R_{1-4}(t)$ (real part of R_1, R_3, R_4 and imaginary part of R_2), defined in eqs. (20, 21), as computed on our lattice. Illustration is provided for $\kappa_Q = 0.1220$ and $\kappa_q = 0.1348$.

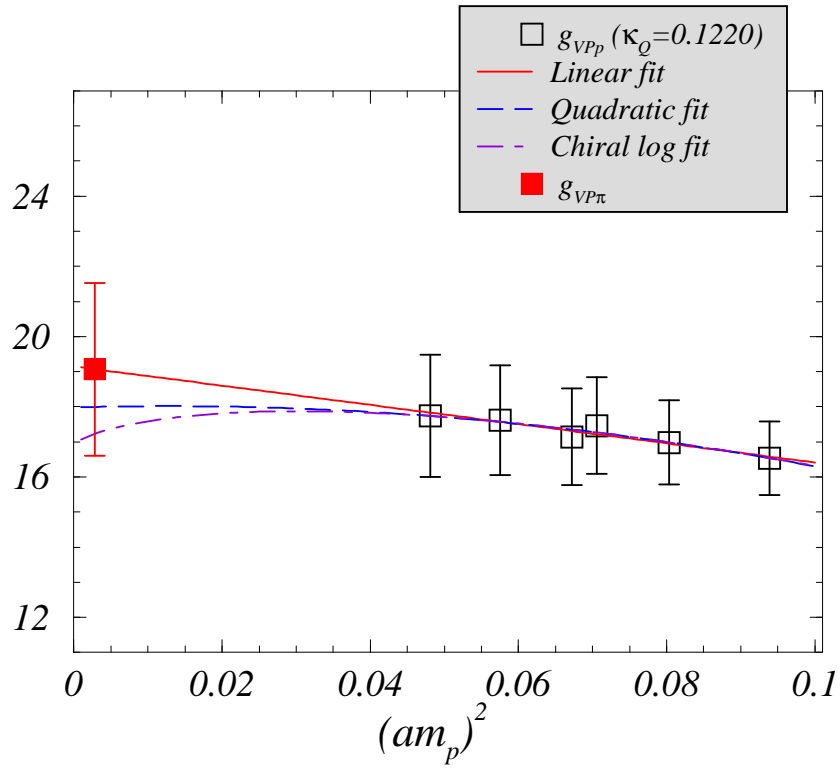


Figure 4: Chiral extrapolation of g_{VPp} without the G_2/G_1 corrections for a fixed heavy quark at $\beta = 6.2$. The curves obtained from the fit to eqs. (26,27,28) are displayed. The filled square point with its error bars corresponds to the linear extrapolation. The complete list of result can be found in table 4.

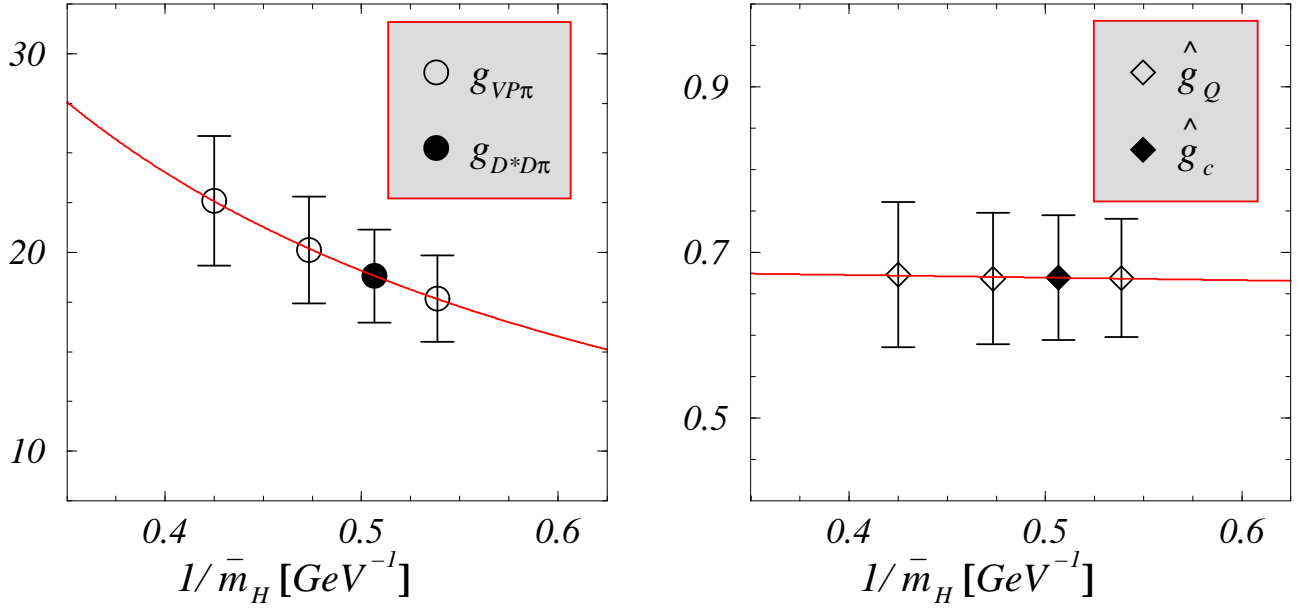


Figure 5: Fit of our data (empty symbols) for $g_{VP\pi}$ and \hat{g}_Q , at $\beta = 6.2$, to the forms (32). The results of interpolation to the \bar{D} -meson is denoted by the filled symbols.

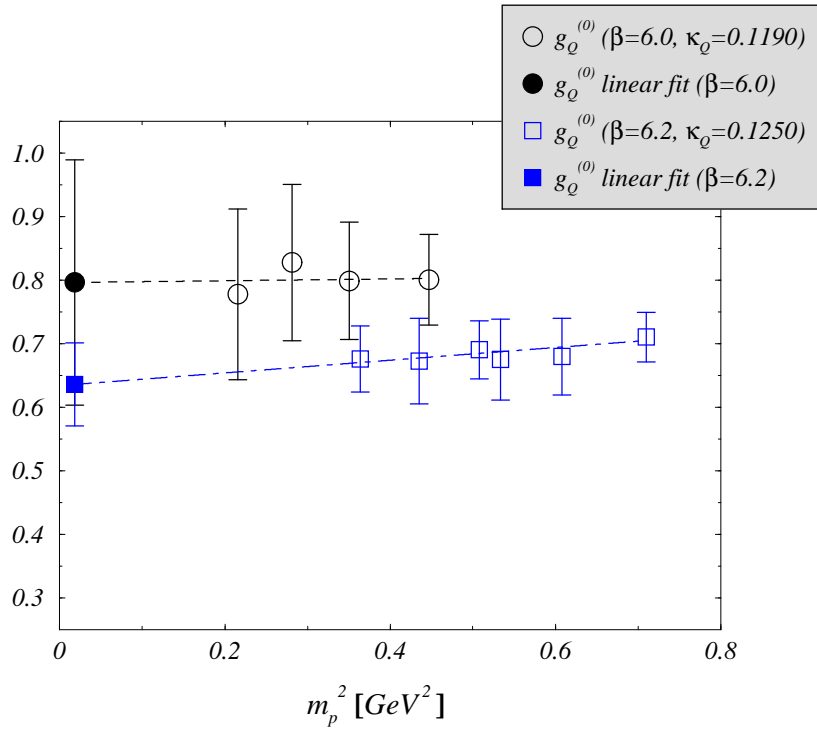


Figure 6: Chiral extrapolation of $\hat{g}_Q^{(0)}$ for a fixed heavy quark $\kappa_Q = 0.1190$ at $\beta = 6.0$ and $\kappa_Q = 0.1250$ at $\beta = 6.2$ corresponding approximately to the same heavy meson mass.

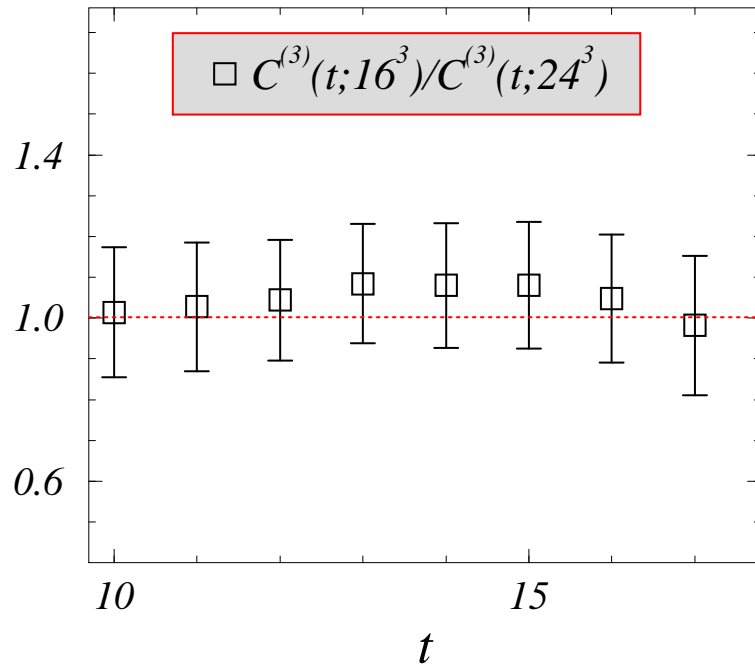


Figure 7: Ratio of the three point functions (19) as obtained for the same meson masses at $\beta = 6.0$ but on different volumes $16^3 \times 64$ and $24^3 \times 64$. Illustrated is the case of the heavy quark corresponding to $\kappa_Q = 0.1220$ and the light ones to $\kappa_q = 0.1344$.